The inhomogeneous RPA and many-electron trial wave functions

R. Gaudoin, M. Nekovee,* and W. M. C. Foulkes
CMTH Group, Blackett Laboratory, Imperial College of Science, Technology and Medicine, Prince Consort Road, London SW7 2BZ, England

R. J. Needs and G. Rajagopal
TCM Group, Cavendish Laboratory, Cambridge University, Madingley Road, Cambridge CB3 0HE
(October 19, 2000)

The long-range electronic correlations in a uniform electron gas may be deduced from the random-phase approximation (RPA) of Bohm and Pines. Here we generalize the RPA to nonuniform systems and use it to derive many-electron Slater-Jastrow trial wave functions for quantum Monte Carlo simulations. The RPA theory fixes the long-range behavior of the inhomogeneous two-body terms in the Jastrow factor and provides an accurate analytic expression for the one-body terms. It also explains the success of Slater-Jastrow trial functions containing determinants of Hartree-Fock or density-functional orbitals, even though these theories do not include Jastrow factors. After adjusting the RPA Jastrow factor to incorporate the known short-range behavior, we test it using variational Monte Carlo. In the small inhomogeneous electron gas system we consider, the analytic RPA-based Jastrow factor slightly outperforms the standard numerically optimized form. The inhomogeneous RPA theory therefore enables us to reduce or even avoid the costly numerical optimization process.

PACS: 71.10.Ca, 71.45.Gm, 02.70.Lq

I. INTRODUCTION

This paper discusses approximate ground-state wave functions for inhomogeneous interacting many-electron systems such as solids. In particular, we consider wave functions of the Slater-Jastrow type, $\Psi = e^J D$, where D is a Slater determinant and J, the Jastrow factor, takes account of the electronic correlations. Our aim is to understand the surprisingly accurate results obtained when Slater-Jastrow trial functions are used in variational quantum Monte Carlo (VQMC) simulations[1,2] of weakly-correlated solids such as silicon. Despite the apparent simplicity of the Slater-Jastrow form, cohesive energies calculated using VQMC are typically an order of magnitude more accurate[3–7] than cohesive energies obtained using Hartree-Fock (HF) or density-functional theory within the local density approximation (LDA).[8]

This is not the place for a general introduction to VQMC (see Hammond *et al.*[2] and Foulkes *et al.*[9] for reviews), but a brief sketch may be helpful. The idea is to obtain an approximate many-electron ground state by numerically optimizing an explicit parametrized trial wave function. The multi-dimensional integrals that give expectation valus are then evaluated using Monte Carlo integration,[10] which scales much more favorably with the dimension than grid-based integration methods.

The trial wave functions used in most QMC simulations contain a Slater determinant of LDA or HF orbitals and a Jastrow factor that includes pairwise correlation terms, $u_{\sigma_i,\sigma_j}(\mathbf{r}_i,\mathbf{r}_j)$, and one-electron terms, $\chi_{\sigma_i}(\mathbf{r}_i)$, where $\mathbf{r}_i$ and σ_i are the position and spin component of electron i. In simulations of solids, it is common to simplify the Jastrow factor by insisting that u be both homogeneous and isotropic (i.e., $u_{\sigma_i,\sigma_j}(\mathbf{r}_i,\mathbf{r}_j)$ is assumed to depend only on the interelectronic distance $r_{ij} = |\mathbf{r}_i - \mathbf{r}_j|$). This approximation works remarkably well, even in strongly inhomogeneous solids. The u and χ functions are usually obtained by optimizing specific parametrized functional forms according to the variational principle.

In this paper we derive a physically-motivated inhomogeneous and anisotropic Jastrow factor for nonuniform systems, based on a generalization of the random-phase approximation (RPA) of Bohm and Pines.[11] This enables us to reduce or even dispense with the time-consuming optimization procedure.

The RPA theory of the *homogeneous* electron gas[11] is often quoted in discussions of Jastrow factors for QMC simulations.[12] Although complicated to derive, the homogeneous RPA has played a central part in the theory of many-electron systems for almost 50 years and has a wide range of applications. In the QMC context, it predicts that the u function should decay like $1/r_{ij}$ for large r_{ij}, but says nothing about the χ function (which is zero in a homogeneous system) or the short-range behavior of u. Although it is easy to modify the u function to make it have the correct cusp-like behavior at short range, the absence of χ terms implies that the homogeneous RPA Jastrow factor produces inaccurate densities, and hence poor energies, when used in strongly inhomogeneous systems. This problem is usually fixed by adding a parametrized χ function and optimizing the parameters numerically.[3]

Here, we generalize the RPA theory to *inhomogeneous* systems (we have recently learned of some unpublished work along similar lines by Fahy and coworkers). The potential applications of the inhomogeneous RPA are at least as numerous as those of the homogeneous RPA, and

so we view this derivation as a central part of the paper. In the homogeneous limit, our approach reduces to that of Bohm and Pines,[11] although with some improvements. In particular, we provide a clearer understanding of the so-called subsidiary condition.

We then apply the inhomogeneous RPA theory to the construction of trial functions for QMC simulations. Some of the results we obtain have been discussed previously by Malatesta[13] and Fahy,[14] who used simple physical arguments to propose a relationship between the u and χ functions. Although these authors pointed out the link to the RPA, they made no attempt to derive it. Here we provide a derivation. Furthermore, the theory we develop gives a complete prescription for u and χ, not just a relationship between them.

The most obvious consequence of the inhomogeneous RPA theory is that it produces a truly inhomogeneous and anisotropic correlation term. The short-range behavior of the inhomogeneous RPA u function is no better than that of the homogeneous version, but is more difficult to correct. We impose the required short-range cusps using a k-space method which, although approximate, works well. Although the inhomogeneities of the RPA u function are significant, the imposition of the cusp conditions makes the u function much more homogeneous. This explains why Slater-Jastrow trial functions incorporating homogeneous u functions describe real solids so well.

Another interesting aspect of the inhomogeneous RPA theory is that it provides a justification for using Slater determinants consisting of LDA or HF orbitals. This is common practice but is not obviously correct: one might guess that the HF orbitals that are optimal in the absence of a Jastrow factor would no longer be accurate in its presence. In fact, the RPA theory shows that HF or LDA orbitals are close to optimal whether or not an RPA Jastrow factor is present.

We test our inhomogeneous RPA Jastrow factor by carrying out VQMC calculations for a strongly inhomogeneous electron gas. We find that the inhomogeneous RPA χ function is of such high quality that there is no need to resort to the standard but costly numerical optimization methods. The small inhomogeneities remaining in the u function after the cusp conditions have been imposed produce a relatively small improvement, but the LDA is so accurate that even this small improvement is $\sim$15% of the difference between the LDA and VQMC ground-state energies. Since the LDA sets the standard that VQMC calculations are supposed to surpass, such a change is physically significant. Other work[15,16] suggests that inhomogeneous u functions are somewhat more effective in full core atoms and molecules.

In summary, the five main results of this paper are:

1. We have extended the RPA to inhomogeneous systems.

2. We have used the inhomogeneous RPA and the cusp conditions to generate accurate inhomogeneous Jastrow factors without numerical optimization. This approach yields a complete, parameter-free prescription for the u and χ functions, not just a relationship between them.

3. We have explained why Slater-Jastrow-type wave functions containing LDA or HF orbitals work so well, and why the use of homogeneous u functions is often sufficient even in strongly inhomogeneous systems.

4. We have developed a method for imposing cusps on inhomogeneous Jastrow factors.

5. We have tested the analytic RPA Jastrow factor in a strongly inhomogeneous electron gas, and found that it slightly outperforms standard numerically optimized Jastrow factors.

The rest of this paper is organized as follows. In Sec. II we describe the Slater-Jastrow trial wave functions used in most QMC simulations of atoms, molecules, and solids. Sec. III presents the RPA theory of the inhomogeneous electron gas, and Sec. IV explains how it leads to Slater-Jastrow trial wave functions containing both χ terms and inhomogeneous u terms. Sec. V discusses the results of the VQMC simulations we have done to test the inhomogeneous RPA Jastrow factor, Sec. VI discusses computational issues, and Sec. VII concludes.

II. TRIAL WAVE FUNCTIONS FOR QMC SIMULATIONS

The aim of this paper is to provide a better physical understanding of the success of the Slater-Jastrow trial wave functions used in many QMC calculations of atoms, molecules, and weakly correlated solids. A Slater-Jastrow trial function is the product of a totally antisymmetric Slater determinant D and a totally symmetric Jastrow factor e^J. When dealing with spin-independent Hamiltonians, the Slater determinant may be split into two smaller determinants, one for each spin value:

$$\Psi = e^J D_\uparrow D_\downarrow \ . \tag{2.1}$$

This reduces the numerical complexity without loss of generality.[17] The orbitals used in $D_\uparrow$ and $D_\downarrow$ are normally obtained from LDA or HF calculations.

The Slater determinants build in exchange effects but neglect the electronic correlations caused by the Coulomb interactions. The most important correlation effects, which occur when pairs of electrons approach each other, may be included by choosing a pairwise Jastrow factor of the form:

$$J = \frac{1}{2}\sum_{i,j} u_{\sigma_i\sigma_j}(\mathbf{r}_i, \mathbf{r}_j) \ . \tag{2.2}$$

The correct short range behaviour of the two-body term can be enforced by introducing spin dependent cusp conditions[18,19] on $u_{\sigma_i\sigma_j}$:

$$\left.\frac{\partial u_{\uparrow\downarrow}(\mathbf{r}_i,\mathbf{r}_j)}{\partial r_{ij}}\right|_{r_{ij}=0} = \frac{1}{2}\ , \quad \left.\frac{\partial u_{\uparrow\uparrow}(\mathbf{r}_i,\mathbf{r}_j)}{\partial r_{ij}}\right|_{r_{ij}=0} = \frac{1}{4}\ . \quad (2.3)$$

These ensure that the local energy $E_L = \hat{H}\Psi/\Psi$, which is the quantity actually sampled in the simulation, does not diverge as r_{ij} approaches zero. (Except where otherwise stated, we use Hartree atomic units, $\hbar = e = 4\pi\varepsilon_0 = m_e = 1$, throughout this paper.)

Because the LDA or HF orbitals in $D_\uparrow$ and $D_\downarrow$ already give a reasonably good approximation to the density, the introduction of a two-body u function usually causes the density of the many-electron wave function to deteriorate. As a result the trial energy deteriorates too. It is therefore necessary to introduce one-body χ terms to adjust the Jastrow factor:

$$e^J = \exp\left(\frac{1}{2}\sum_{i,j} u_{\sigma_i\sigma_j}(\mathbf{r}_i,\mathbf{r}_j) + \sum_i \chi_{\sigma_i}(\mathbf{r}_i)\right)\ . \quad (2.4)$$

Note the sign conventions here: our definition of u is the negative of that used by many other authors. Most authors also omit the diagonal $i = j$ terms in the sum over i and j. In homogeneous systems the diagonal terms only affect the normalization of the trial function, while in inhomogeneous systems they add one-body contributions that may be accounted for by redefining $\chi_\sigma(\mathbf{r})$.

Since we are using periodic boundary conditions, it is often convenient to express the χ function, the electron density, and the Jastrow factor in reciprocal space. We use symmetric definitions of the Fourier transformations,

$$f(\mathbf{k}) = \frac{1}{\sqrt{V}}\int_V f(\mathbf{r})e^{i\mathbf{k}\cdot\mathbf{r}}d^3r\ , \quad (2.5)$$

$$g(\mathbf{k},\mathbf{k}') = \frac{1}{V}\int_V e^{i\mathbf{k}\cdot\mathbf{r}}g(\mathbf{r},\mathbf{r}')e^{-i\mathbf{k}'\cdot\mathbf{r}'}d^3rd^3r', \quad (2.6)$$

with back transformations $f(\mathbf{r}) = V^{-1/2}\sum_{\mathbf{k}} f(\mathbf{k})e^{-i\mathbf{r}\cdot\mathbf{k}}$ and $g(\mathbf{r},\mathbf{r}') = V^{-1}\sum_{\mathbf{k},\mathbf{k}'} e^{-i\mathbf{r}\cdot\mathbf{k}}g(\mathbf{k},\mathbf{k}')e^{i\mathbf{r}'\cdot\mathbf{k}'}$.

Several different types of Jastrow factor are in common use, the best known of which[12] is based on the RPA of Bohm and Pines.[11] Others are based on the RPA in the form due to Gaskell[20] or the Fermi hypernetted chain approximation.[21] For extra accuracy, most Jastrow factors incorporate a number of variational parameters that are optimized numerically.[22,23]

A. The homogeneous RPA correlation term

As will be explained in Sec. IV, the RPA theory of Bohm and Pines[11] suggests that the long-range behavior of the correlation term u in a homogeneous electron gas of number density n should take the form:

$$u_{\sigma_i\sigma_j}(\mathbf{r}_i,\mathbf{r}_j) = u_{\sigma_i\sigma_j}(r_{ij}) = -\frac{1}{\omega_p r_{ij}}\ , \quad (2.7)$$

where $\omega_p = \sqrt{4\pi n}$ is the plasma frequency. This spin-independent two-body term has no cusp and is only expected to be correct for large r_{ij}. Multiplying Eq. (2.7) by $1-\exp(-r_{ij}/F_{\sigma_i\sigma_j})$ yields

$$u_{\sigma_i\sigma_j}(r_{ij}) = -\frac{1}{\omega_p r_{ij}}\left(1-e^{-r_{ij}/F_{\sigma_i\sigma_j}}\right)\ , \quad (2.8)$$

which approaches Eq. (2.7) for large r_{ij} and also has the correct cusp behavior if $F_{\sigma_i\sigma_j}$ is chosen appropriately.

B. The χ function

The χ function needed to counteract the density-altering effects of the u function is normally obtained by numerical optimization. To avoid this costly procedure we can use the result of Sec. III and include a one-body term of the form:

$$\chi_\sigma(\mathbf{k}) = -\sum_{\mathbf{k}',\sigma'} u_{\sigma\sigma'}(\mathbf{k},\mathbf{k}')n_{\sigma'}(\mathbf{k}')\ . \quad (2.9)$$

If the u function is homogeneous, $u_{\sigma\sigma'}(\mathbf{r},\mathbf{r}') = u_{\sigma\sigma'}(\mathbf{r}-\mathbf{r}')$, this reduces to

$$\chi_\sigma(\mathbf{k}) = -\sqrt{V}\sum_{\sigma'} u_{\sigma\sigma'}(\mathbf{k})n_{\sigma'}(\mathbf{k}) \quad (2.10)$$

as derived by Malatesta.*et al.*[13] Strictly speaking, however, the u function is only homogeneous when the electron density is homogeneous, and hence when $\chi = 0$.

III. THE RANDOM-PHASE APPROXIMATION FOR INHOMOGENEOUS SYSTEMS

This section generalizes the standard RPA treatment of homogeneous systems[11,24,25] to inhomogeneous systems. As we are interested in describing the long-range correlations due to the electron-electron interaction, we wish to make a connection between the Hamiltonian and the long wavelength density fluctuations known as plasmons. Our eventual aim is to split the Hamiltonian into an electronic term with short-range interactions and a plasmon term that is only weakly coupled to the electrons. Once the electron and plasmon parts of the Hamiltonian have been (almost) decoupled in this way, we shall see that the long-range correlations are described by the ground-state wave function of the plasmon part, which is simply a set of quantum mechanical harmonic oscillators. At shorter wavelengths the plasmons are not well defined and the collective plasmon description of electronic correlation ceases to be valid. Instead, the electrons feel a short-range screened interaction that produces additional electron-electron scattering-like correlations.

The assumption of weak plasmon-electron interaction is reasonable at small k since long wavelength plasmons are long lived. For larger k values the almost flat plasmon dispersion curve runs into the continuum of electron-hole pair excitations and the plasmons are no longer well defined. In a uniform electron gas this happens at a wave vector k_c given by[25]

$$k_c \approx \frac{1}{2} k_F r_s^{1/2} \propto n^{1/6} \,, \tag{3.1}$$

where k_F is the Fermi wave vector, $r_s a_0$ is the radius of a sphere containing one electron on average, and a_0, the Bohr radius, is the atomic unit of length. This estimate of the cutoff should also be applicable to inhomogeneous systems as long as the density does not vary too much. We see that for typical metals with r_s values of 2 or 3 the cutoff is of the order of the Fermi wave vector.

A. Orientation

The RPA is a sophisticated theory and the derivation is complicated even in the homogeneous case.[11] The inhomogeneous generalization presented here clarifies certain aspects, but also introduces extra subtleties. To help orient readers, here is a brief summary of the steps to follow:

1. Extra degrees of freedom are added to the many-electron Hamiltonian. Although these operate in a separate Hilbert space, they will later become linked to the plasmons.

2. It is shown that the parameters of the extended Hamiltonian may be chosen such that its ground state is simply related to that of the original Hamiltonian. This choice of parameters may be viewed as the imposition of a subsidiary condition on the extra degrees of freedom.

3. After applying a unitary transformation, the extended Hamiltonian is approximated as a sum of two decoupled Hamiltonians (this is the random phase approximation). One of the decoupled Hamiltonians acts in the original Hilbert space, the other in the Hilbert space of the additional degrees of freedom.

4. The part of the decoupled Hamiltonian involving the additional degrees of freedom is a set of harmonic oscillators, the frequencies of which correspond to the plasmon energies. A straightforward analysis (not included here) shows that the subsidiary condition links the momentum and position operators occurring in these harmonic oscillators to the electric field and longitudinal vector potential of the inhomogeneous electron gas.

5. The approximate RPA Hamiltonian yields an approximate ground-state wave function. After inverting the unitary transformation, it is then possible to extract an approximate ground state of the original Hamiltonian. This has the Slater-Jastrow form including both an inhomogeneous u function and a χ function.

B. The RPA Hamiltonian in inhomogeneous systems

The aim is to find an approximate ground state $|\psi_0\rangle$ with energy E_0 of the following Hamiltonian:

$$\hat{H} = \frac{1}{2}\sum_i \hat{\mathbf{p}}_i^2 + \sum_i V(\hat{\mathbf{r}}_i) + 2\pi \sum_{\mathbf{k}} \frac{\hat{n}_{\mathbf{k}}\hat{n}_{\mathbf{k}}^\dagger}{k^2} - \frac{2\pi N}{V}\sum_{\mathbf{k}} \frac{1}{k^2} \,, \tag{3.2}$$

where $V(\mathbf{r})$ is an applied potential. Note that we adopt a slightly unusual definition of the number density operator,

$$\hat{n}_{\mathbf{k}} = \frac{1}{\sqrt{V}} \sum_i e^{i\mathbf{k}\cdot\hat{\mathbf{r}}_i} \,, \tag{3.3}$$

which includes a $1/\sqrt{V}$ factor in accord with the symmetric definition of the Fourier transform used throughout this paper. The system is assumed to be charge neutral and so the $\mathbf{k} = 0$ terms are omitted from all k-space summations.

The "physical" Hilbert space in which this Hamiltonian acts will be denoted $\mathcal{H}_R$. For reasons that will become clear later on, it is convenient to rewrite $\hat{H}$ in the form,

$$\hat{H} = \frac{1}{2}\sum_i \hat{\mathbf{p}}_i^2 + \sum_i \tilde{V}(\hat{\mathbf{r}}_i) + 2\pi \sum_{\mathbf{k}} \frac{\hat{n}_{\mathbf{k}}\hat{n}_{\mathbf{k}}^\dagger}{k^2} - \frac{2\pi N}{V}\sum_{\mathbf{k}} \frac{1}{k^2} + \frac{1}{2}\sum_{k<k_c} \pi_{\mathbf{k}}^0 \pi_{-\mathbf{k}}^0 - \sum_{k<k_c} \left(\frac{4\pi}{k^2}\right)^{1/2} \pi_{\mathbf{k}}^0 \hat{n}_{\mathbf{k}}^\dagger \,, \tag{3.4}$$

where $\tilde{V}(\mathbf{r})$ is defined via:

$$\tilde{V}(\mathbf{r}) = V(\mathbf{r}) - \frac{\Delta E}{N} - \Delta V(\mathbf{r}) \,, \tag{3.5}$$

$$\Delta E = \frac{1}{2}\sum_{k<k_c} \pi_{\mathbf{k}}^0 \pi_{-\mathbf{k}}^0 \,, \tag{3.6}$$

$$\Delta V(\mathbf{r}) = -\sum_{k<k_c} \left(\frac{4\pi}{k^2}\right)^{1/2} \pi_{\mathbf{k}}^0 \frac{e^{-i\mathbf{k}\cdot\mathbf{r}}}{\sqrt{V}} \,, \tag{3.7}$$

the $\pi^0_{\mathbf{k}}$ are arbitrary numbers satisfying ${\pi^0_{\mathbf{k}}}^* = \pi^0_{-\mathbf{k}}$, and k_c is the plasmon cutoff from Eq. (3.1).

Let us now introduce conjugate pairs of operators, $\hat{\pi}_{\mathbf{k}}$ and $\hat{q}_{\mathbf{k}}$, acting in a different Hilbert space $\mathcal{H}_O$, which we call the oscillator space. The "momentum" operator $\hat{\pi}_{\mathbf{k}}$ and the "position" operator $\hat{q}_{\mathbf{k}}$ are taken to be the Fourier transforms of field operators $\hat{\pi}(\mathbf{r}) = \hat{\pi}^\dagger(\mathbf{r})$ and $\hat{q}(\mathbf{r}) = \hat{q}^\dagger(\mathbf{r})$:

$$\hat{q}^\dagger_{\mathbf{k}} = \frac{1}{\sqrt{V}} \int_V e^{i\mathbf{k}\cdot\mathbf{r}} \hat{q}^\dagger(\mathbf{r}) d^3r \;, \tag{3.8}$$

$$\hat{\pi}_{\mathbf{k}} = \frac{1}{\sqrt{V}} \int_V e^{i\mathbf{k}\cdot\mathbf{r}} \hat{\pi}(\mathbf{r}) d^3r \;, \tag{3.9}$$

which satisfy the standard canonical commutation relation $[\hat{\pi}(\mathbf{r}), \hat{q}(\mathbf{r}')] = -i\delta(\mathbf{r}-\mathbf{r}')$. It therefore follows that $\hat{\pi}^\dagger_{\mathbf{k}} = \hat{\pi}_{-\mathbf{k}}$ and $\hat{q}^\dagger_{\mathbf{k}} = \hat{q}_{-\mathbf{k}}$ obey

$$[\hat{\pi}_{\mathbf{k}}, \hat{q}_{\mathbf{k}'}] = -i\delta_{\mathbf{k},\mathbf{k}'} \;. \tag{3.10}$$

For the time being $\hat{\pi}_{\mathbf{k}}$ and $\hat{q}_{\mathbf{k}}$ have little physical meaning, but later in the derivation they will become associated with the plasmon coordinates.

Now consider the Hermitian *extended Hamiltonian*,

$$\begin{aligned}\hat{H}_{\rm BP} = &\frac{1}{2}\sum_i \hat{\mathbf{p}}_i^2 + \sum_i \tilde{V}(\hat{\mathbf{r}}_i) \\ &+ 2\pi \sum_{\mathbf{k}} \frac{\hat{n}_{\mathbf{k}}\hat{n}^\dagger_{\mathbf{k}}}{k^2} - \frac{2\pi N}{V}\sum_{\mathbf{k}}\frac{1}{k^2} \\ &+ \frac{1}{2}\sum_{k<k_c} \hat{\pi}_{\mathbf{k}}\hat{\pi}_{-\mathbf{k}} - \sum_{k<k_c}\left(\frac{4\pi}{k^2}\right)^{1/2} \hat{\pi}_{\mathbf{k}}\hat{n}^\dagger_{\mathbf{k}} \;,\end{aligned} \tag{3.11}$$

which is an operator in the extended Hilbert space $\mathcal{H}_{\rm ext} = \mathcal{H}_R \bigotimes \mathcal{H}_O$. Note that the potential $\tilde{V}$ is still the same as given by Eq. (3.5); the variables $\pi^0_{\mathbf{k}}$ that were used to construct $\tilde{V}$ have not been replaced by operators in $\mathcal{H}_O$, but remain ordinary complex numbers. Because $\hat{H}_{\rm BP}$ and $\hat{\boldsymbol{\pi}}$ commute they may be diagonalized simultaneously, and hence all eigenstates of the extended Hamiltonian $\hat{H}_{\rm BP}$ may be written in the form $|\psi_{\boldsymbol{\pi}}\rangle|\boldsymbol{\pi}\rangle$, where $\hat{\pi}_{\mathbf{k}}|\boldsymbol{\pi}\rangle = \pi_{\mathbf{k}}|\boldsymbol{\pi}\rangle$ for all $k < k_c$.

Let $|\psi_0\rangle$ and E_0 be the ground-state wave function and ground-state eigenvalue of the physical Hamiltonian $\hat{H}$. If we define an eigenstate $|\boldsymbol{\pi}^0\rangle$ of the $\hat{\pi}_{\mathbf{k}}$ operators such that $\hat{\pi}_{\mathbf{k}}|\boldsymbol{\pi}^0\rangle = \pi^0_{\mathbf{k}}|\boldsymbol{\pi}^0\rangle$ for all $k < k_c$, it follows that $|\psi_0\rangle|\boldsymbol{\pi}^0\rangle$ is an eigenstate of $\hat{H}_{\rm BP}$ with the same eigenvalue E_0. It need not, however, be the ground state of $\hat{H}_{\rm BP}$, which might correspond to a different wave function $|\psi_{\rm min}\rangle|\boldsymbol{\pi}^{\rm min}\rangle$. The question that now arises is how to choose the constants $\pi^0_{\mathbf{k}}$ (and hence the modified potential $\tilde{V}$) such that $|\psi_0\rangle|\boldsymbol{\pi}^0\rangle$ is in fact the ground state of $\hat{H}_{\rm BP}$ and not just some other eigenstate. This can be achieved using the Hellmann-Feynman theorem.

Consider the lowest energy state $|\Phi_{\boldsymbol{\pi}}\rangle = |\psi_{\boldsymbol{\pi}}\rangle|\boldsymbol{\pi}\rangle$ corresponding to some fixed oscillator-space eigenstate $|\boldsymbol{\pi}\rangle$. The energy eigenvalue of $|\Phi_{\boldsymbol{\pi}}\rangle$ will be denoted $E^{\boldsymbol{\pi}}$. When $\hat{H}_{\rm BP}$ acts on $|\Phi_{\boldsymbol{\pi}}\rangle$, the operators $\hat{\pi}_{\mathbf{k}}$ may be replaced by their eigenvalues $\pi_{\mathbf{k}}$, and hence $|\psi_{\boldsymbol{\pi}}\rangle$ is in fact the ground state of

$$\begin{aligned}\hat{H}^{\boldsymbol{\pi}} = &\frac{1}{2}\sum_i \hat{\mathbf{p}}_i^2 + \sum_i \tilde{V}(\hat{\mathbf{r}}_i) \\ &+ 2\pi \sum_{\mathbf{k}} \frac{\hat{n}_{\mathbf{k}}\hat{n}^\dagger_{\mathbf{k}}}{k^2} - \frac{2\pi N}{V}\sum_{\mathbf{k}}\frac{1}{k^2} \\ &+ \frac{1}{2}\sum_{k<k_c} \pi_{\mathbf{k}}\pi_{-\mathbf{k}} - \sum_{k<k_c}\left(\frac{4\pi}{k^2}\right)^{1/2} \pi_{\mathbf{k}}\hat{n}^\dagger_{\mathbf{k}} \;.\end{aligned} \tag{3.12}$$

Note that $\hat{H}^{\boldsymbol{\pi}}$ operates not in the extended Hilbert space but in $\mathcal{H}_R$. Furthermore, it is important to keep in mind that $\tilde{V}$ is formed using the as yet unknown numbers $\pi^0_{\mathbf{k}}$. The overall ground state of $\hat{H}_{\rm BP}$ corresponds to the minimum of $E^{\boldsymbol{\pi}}$ with respect to $\boldsymbol{\pi}$. As we are now looking at a standard quantum mechanical problem formulated in the physical Hilbert space $\mathcal{H}_R$, the Hellmann-Feynman theorem gives:

$$\frac{\partial E^{\boldsymbol{\pi}}}{\partial \pi_{\mathbf{k}}} = \left\langle \psi_{\boldsymbol{\pi}} \left| \frac{\partial \hat{H}^{\boldsymbol{\pi}}}{\partial \pi_{\mathbf{k}}} \right| \psi_{\boldsymbol{\pi}} \right\rangle \tag{3.13}$$

$$= \pi_{-\mathbf{k}} - \left(\frac{4\pi}{k^2}\right)^{1/2} \langle \psi_{\boldsymbol{\pi}} | \hat{n}^\dagger_{\mathbf{k}} | \psi_{\boldsymbol{\pi}} \rangle \;, \tag{3.14}$$

where $|\psi_{\boldsymbol{\pi}}\rangle$ is assumed normalized. If the overall ground state of $\hat{H}_{\rm BP}$ occurs when $\boldsymbol{\pi} = \boldsymbol{\pi}^{\rm min}$, it follows that:

$$0 = \pi^{\rm min}_{-\mathbf{k}} - \left(\frac{4\pi}{k^2}\right)^{1/2} \langle \psi_{\boldsymbol{\pi}^{\rm min}} | \hat{n}^\dagger_{\mathbf{k}} | \psi_{\boldsymbol{\pi}^{\rm min}} \rangle \;. \tag{3.15}$$

Eq. (3.15) is the generalization to inhomogeneous systems of the "subsidiary condition" of Bohm and Pines.[11] It can be rewritten as

$$\hat{\Omega}_{\mathbf{k}}|\Phi\rangle = 0 \qquad (k < k_c), \tag{3.16}$$

where

$$\hat{\Omega}_{\mathbf{k}} = \hat{\pi}_{\mathbf{k}} - \left(\frac{4\pi}{k^2}\right)^{1/2} \langle \hat{n}_{\mathbf{k}} \rangle_0 \hat{1} \;, \tag{3.17}$$

and has to be obeyed by $|\Phi_0\rangle$, the exact ground state of $\hat{H}_{\rm BP}$. In the case of a homogeneous system, Eq. (3.16) reduces to $\hat{\pi}_{\mathbf{k}}|\Phi\rangle = 0$ as derived using a different method by Bohm and Pines.[11] Note that the subsidiary condition is not a prescription for the replacement of one variable by another, as stated by Bohm and Pines;[11] instead, it characterizes a property of the ground state of $\hat{H}_{\rm BP}$ that aids us in devising approximations.

We wish to choose the constants $\pi^0_{\mathbf{k}}$ such that $\pi^0_{\mathbf{k}} = \pi^{\rm min}_{\mathbf{k}}$, since in this case we have already argued that the physical-space part $|\psi_{\boldsymbol{\pi}^0}\rangle$ of the Bohm-Pines ground state

$$|\Phi_{\boldsymbol{\pi}^0}\rangle = |\psi_{\boldsymbol{\pi}^0}\rangle|\boldsymbol{\pi}^0\rangle \tag{3.18}$$

is equal to the exact physical ground state $|\psi_0\rangle$. The sought after link between $|\psi_0\rangle$ and the $\pi^0_{\mathbf{k}}$ is therefore:

$$\pi^0_{-\mathbf{k}} = \left(\frac{4\pi}{k^2}\right)^{1/2} \langle\psi_0|\hat{n}^\dagger_{\mathbf{k}}|\psi_0\rangle = \left(\frac{4\pi}{k^2}\right)^{1/2} \langle\hat{n}_{-\mathbf{k}}\rangle_0 \ , \quad (3.19)$$

where $\langle\hat{n}_{\mathbf{k}}\rangle_0 = \langle\psi_0|\hat{n}_{\mathbf{k}}|\psi_0\rangle$ is a Fourier component of the ground-state electron density $n(\mathbf{r})$. Note that Eq. (3.19) is *not* an operator equation; it simply links one number, $\pi^0_{-\mathbf{k}}$, to another, $\langle\hat{n}_{-\mathbf{k}}\rangle_0$. Since all the $\hat{\pi}_{\mathbf{k}}$ operators have $k < k_c$, Eq. (3.19) only applies when $k < k_c$.

More generally, if we have set the parameters $\pi^0_{\mathbf{k}}$ using Eq. (3.19), the physical-space parts $|\psi_{\boldsymbol{\pi}}\rangle$ of all extended-space eigenstates $|\Phi_{\boldsymbol{\pi}}\rangle = |\psi_{\boldsymbol{\pi}}\rangle|\boldsymbol{\pi}\rangle$ that obey the subsidiary condition, Eq. (3.16), are eigenstates of the original Hamiltonian, Eq. (3.2). This follows from the definition of the potential $\tilde{V}(\mathbf{r})$, which is such that the Hamiltonian in Eq. (3.12) is the same as the original Hamiltonian of Eq. (3.2) when the value of $\boldsymbol{\pi}$ is consistent with the subsidiary condition: $\hat{H}^{\boldsymbol{\pi}}\,|_{\pi_{\mathbf{k}}=\pi^0_{\mathbf{k}}} = \hat{H}$.

Eq. (3.19) specifies $\pi^0_{\mathbf{k}}$ in terms of the ground-state density, which is obtained by solving $\hat{H}_{\rm BP}$. Unfortunately, this Hamiltonian depends on the parameters $\pi^0_{\mathbf{k}}$ calculated from its ground state, and so we are faced with a self-consistency problem analogous to those encountered in bandstructure calculations. However, as we only need the ground-state density, and as it is known that the LDA gives reasonably good ground-state densities in most solids, we can in practice use the LDA density $\langle\hat{n}_{\mathbf{k}}\rangle_0^{\rm LDA}$ to obtain a good approximation for $\pi^0_{\mathbf{k}}$.

Let us now use the subsidiary condition to evaluate ΔE and $\Delta V(\mathbf{r})$. For ΔE we get

$$\begin{aligned}\Delta E &= \frac{1}{2}\sum_{k<k_c}\frac{4\pi}{k^2}\langle\hat{n}_{\mathbf{k}}\rangle_0\langle\hat{n}_{-\mathbf{k}}\rangle_0 \\ &= \frac{1}{2}\int\frac{n^l(\mathbf{r})n^l(\mathbf{r}')}{|\mathbf{r}-\mathbf{r}'|}d^3r d^3r' \ , \end{aligned} \quad (3.20)$$

where $n^l(\mathbf{r})$ is the long wavelength ($k < k_c$) part of the ground-state electron density. The constant ΔE is therefore the long wavelength contribution to the Hartree energy. For ΔV we get

$$\Delta V(\mathbf{r}) = -\frac{1}{\sqrt{V}}\sum_{k<k_c}\frac{4\pi}{k^2}\langle\hat{n}_{\mathbf{k}}\rangle_0 e^{-i\mathbf{kr}} \ , \quad (3.21)$$

and hence $\Delta V(\mathbf{r})$ is the Hartree potential corresponding to the long wavelength Fourier components of the electronic charge density. Because $\Delta V(\mathbf{r})$ is subtracted from $V(\mathbf{r})$ to give $\tilde{V}(\mathbf{r})$, the extended Hamiltonian $\hat{H}_{\rm BP}$ contains a reduced external potential. The long-range part of the mutual repulsion of the electrons has been absorbed into the plasmon degrees of freedom via the subsidiary condition.

C. The unitary transformation

We have now concluded that we can concentrate on the ground state of the Bohm-Pines Hamiltonian, $\hat{H}_{\rm BP}$, from Eq. (3.11) instead of the ground state of the original Hamiltonian from Eq. (3.2).

Unsurprisingly, the Bohm-Pines extended Hamiltonian cannot be solved exactly. It may, however, be solved approximately by means of a unitary transformation.[11] We use the unitary operator

$$\hat{S} = \exp\left[-i\sum_{k<k_c}\left(\frac{4\pi}{k^2}\right)^{1/2}\hat{q}_{\mathbf{k}}\hat{n}_{\mathbf{k}}\right] \quad (3.22)$$

to transform an eigenstate $|\Phi\rangle$ of $\hat{H}_{\rm BP}$ into an eigenstate $|\Phi^{\rm new}\rangle = \hat{S}|\Phi\rangle$ of the transformed Hamiltonian $\hat{H}^{\rm new}_{\rm BP} = \hat{S}\hat{H}_{\rm BP}\hat{S}^\dagger$. The position operators $\hat{\mathbf{r}}_i$ and $\hat{q}_{\mathbf{k}}$ are unchanged by the transformation because they commute with $\hat{S}$, but the momentum operators transform as follows:

$$\hat{\mathbf{p}}_i \to \hat{\mathbf{p}}^{\rm new}_i = \hat{\mathbf{p}}_i + i\left(\frac{4\pi}{V}\right)^{1/2}\sum_{k<k_c}\hat{q}_{\mathbf{k}}\boldsymbol{\varepsilon}_{\mathbf{k}}e^{i\mathbf{k}\cdot\hat{\mathbf{r}}_i} \ , \quad (3.23)$$

$$\hat{\pi}_{\mathbf{k}} \to \hat{\pi}^{\rm new}_{\mathbf{k}} = \hat{\pi}_{\mathbf{k}} + \left(\frac{4\pi}{k^2}\right)^{1/2}\hat{n}_{\mathbf{k}} \ , \quad (3.24)$$

where $\boldsymbol{\varepsilon}_{\mathbf{k}} = \mathbf{k}/k$ is a unit vector in the $\mathbf{k}$ direction.

The final result of the unitary transformation defined by Eq. (3.22) is the Hamiltonian:

$$\begin{aligned}\hat{H}^{\rm new}_{\rm BP} &= \frac{1}{2}\sum_i\hat{\mathbf{p}}_i^2 + 2\pi\sum_{k>k_c}\frac{\hat{n}_{\mathbf{k}}\hat{n}^\dagger_{\mathbf{k}}}{k^2} \\ &- \frac{2\pi N}{V}\sum_{\mathbf{k}}\frac{1}{k^2} + \sum_i\tilde{V}(\hat{\mathbf{r}}_i) \\ &+ i\left(\frac{4\pi}{V}\right)^{1/2}\sum_{k<k_c}\sum_i\boldsymbol{\varepsilon}_{\mathbf{k}}\cdot\left(\hat{\mathbf{p}}_i - \frac{\mathbf{k}}{2}\right)\hat{q}_{\mathbf{k}}e^{i\mathbf{k}\cdot\hat{\mathbf{r}}_i} \\ &+ \frac{2\pi}{\sqrt{V}}\sum_{k,k'<k_c}(\boldsymbol{\varepsilon}_{\mathbf{k}}\cdot\boldsymbol{\varepsilon}_{\mathbf{k}'})\,\hat{q}_{\mathbf{k}}\hat{q}_{-\mathbf{k}'}\hat{n}_{\mathbf{k}-\mathbf{k}'} \\ &+ \frac{1}{2}\sum_{k<k_c}\hat{\pi}_{\mathbf{k}}\hat{\pi}_{-\mathbf{k}} \ , \end{aligned} \quad (3.25)$$

which is obtained by replacing $\hat{\mathbf{p}}_i$ and $\hat{\pi}_{\mathbf{k}}$ in Eq. (3.11) by $\hat{\mathbf{p}}^{\rm new}_i$ and $\hat{\pi}^{\rm new}_{\mathbf{k}}$. The subsidiary condition becomes

$$\hat{\Omega}^{\rm new}_{\mathbf{k}}|\Phi^{\rm new}\rangle = 0 \qquad (k < k_c) \ , \quad (3.26)$$

where

$$\hat{\Omega}^{\rm new}_{\mathbf{k}} = \hat{\pi}_{\mathbf{k}} + \left(\frac{4\pi}{k^2}\right)^{1/2}(\hat{n}_{\mathbf{k}} - \langle\hat{n}_{\mathbf{k}}\rangle_0) \ . \quad (3.27)$$

We now make the random-phase approximation, which amounts to replacing the $\hat{n}_{\mathbf{k}-\mathbf{k}'} = V^{-1/2}\sum_i e^{i(\mathbf{k}-\mathbf{k}')\cdot\hat{\mathbf{r}}_i}$

factor in the fourth line of Eq. (3.25) by its ground-state expectation value. In uniform systems the electronic positions $\mathbf{r}_i$ are random and so the phases are also random; the expectation value of $\hat{n}_{\mathbf{k}-\mathbf{k}'}$ is therefore equal to $N\delta_{\mathbf{k},\mathbf{k}'}/\sqrt{V}$. In inhomogeneous systems we have to evaluate the expectation value of the (untransformed) operator $\hat{n}_{\mathbf{k}-\mathbf{k}'}$ in the transformed ground state $|\Phi^{\rm new}\rangle$. Since the density operator $\hat{n}(\mathbf{r}) = \sum_i \delta(\hat{\mathbf{r}}_i - \mathbf{r})$ commutes with the unitary transformation, it follows that

$$\langle\Phi^{\rm new}|\hat{n}(\mathbf{r})|\Phi^{\rm new}\rangle = \langle\Phi|\hat{S}^\dagger\hat{n}(\mathbf{r})\hat{S}|\Phi\rangle = \langle\Phi|\hat{n}(\mathbf{r})|\Phi\rangle \ . \tag{3.28}$$

The required expectation value of $\hat{n}_{\mathbf{k}-\mathbf{k}'}$ is therefore equal to the Fourier component $\langle\hat{n}_{\mathbf{k}-\mathbf{k}'}\rangle_0$ of the ground-state electron density of the original (untransformed) Bohm-Pines Hamiltonian from Eq. (3.11).

Following Bohm and Pines,[11] the plasmon-electron coupling term on the third line of Eq. (3.25) will also be neglected. To justify this approximation (and indeed the RPA) we can appeal to the measured physical properties of interacting electron gases; we know that the plasmons are well defined when $k < k_c$, and hence that the plasmon-electron coupling terms must indeed be small.

IV. THE GROUND-STATE WAVE FUNCTION

This section explains how the inhomogeneous RPA theory introduced above leads to approximate ground-state wave functions of the Slater-Jastrow type, and shows that the use of Slater determinants of LDA or HF orbitals is close to optimal even in the presence of the RPA Jastrow factor. The RPA u and χ functions depend on the electron density and are closely related to each other.

A. The RPA ground state

The two approximations described above decouple the electrons and plasmons and reduce the transformed Hamiltonian of Eq. (3.25) to the RPA Hamiltonian $\hat{H}_{\rm RPA} = \hat{H}_{sr} + \hat{H}_p$. The first two lines of Eq. (3.25) yield the short-range electronic Hamiltonian,

$$\begin{aligned}\hat{H}_{sr} = &\frac{1}{2}\sum_i \hat{\mathbf{p}}_i^2 + 2\pi\sum_{k>k_c}\frac{\hat{n}_{\mathbf{k}}\hat{n}_{\mathbf{k}}^\dagger}{k^2} \\ &-\frac{2\pi N}{V}\sum_{\mathbf{k}}\frac{1}{k^2} + \sum_i \tilde{V}(\hat{\mathbf{r}}_i) \ ,\end{aligned} \tag{4.1}$$

and the last two lines yield the plasmon Hamiltonian,

$$\hat{H}_p = \frac{1}{2}(\hat{\boldsymbol{\pi}}\cdot\hat{\boldsymbol{\pi}}^\dagger + \hat{\mathbf{q}}\cdot M\cdot\hat{\mathbf{q}}^\dagger) \ , \tag{4.2}$$

where the matrix M is given by

$$M_{\mathbf{k},\mathbf{k}'} = (\boldsymbol{\varepsilon}_{\mathbf{k}}\cdot\boldsymbol{\varepsilon}_{\mathbf{k}'})\frac{1}{V}\int e^{i(\mathbf{k}-\mathbf{k}')\cdot\mathbf{r}}\omega_p^2(\mathbf{r})d^3r \ , \tag{4.3}$$

and we have introduced a position dependent local plasma frequency defined by $\omega_p^2(\mathbf{r}) = 4\pi n(\mathbf{r})$. The full ground state of $\hat{H}_{\rm RPA}$ is the product of the ground states of $\hat{H}_{sr}$ and $\hat{H}_p$.

If we choose to work in a representation in which the $\hat{\pi}_{\mathbf{k}}$ operators are diagonal, the plasmon ground state takes the standard simple harmonic oscillator form:

$$\Psi_p \propto \exp\left[-\frac{1}{2}\sum_{k,k'<k_c}\pi_{\mathbf{k}}^*\left(M^{-1/2}\right)_{\mathbf{k},\mathbf{k}'}\pi_{\mathbf{k}'}\right] \ . \tag{4.4}$$

Making use of the expression for $\tilde{V}$ from Eq. (3.5) and the condition $\pi_{\mathbf{k}}^0 = \sqrt{4\pi/k^2}\langle\hat{n}_{\mathbf{k}}\rangle_0$ from Eq. (3.19), the short-range Hamiltonian of Eq. (4.1) becomes:

$$\begin{aligned}\hat{H}_{sr} = &\frac{1}{2}\sum_i\hat{\mathbf{p}}_i^2 + \sum_i V(\hat{\mathbf{r}}_i) \\ &+ 2\pi\sum_{k>k_c}\frac{\hat{n}_{\mathbf{k}}\hat{n}_{\mathbf{k}}^\dagger}{k^2} - \frac{2\pi N}{V}\sum_{\mathbf{k}}\frac{1}{k^2} \\ &+ \frac{1}{\sqrt{V}}\sum_i\sum_{k<k_c}\frac{4\pi\langle\hat{n}_{\mathbf{k}}\rangle_0}{k^2}e^{-i\mathbf{k}\cdot\hat{\mathbf{r}}_i} \\ &- 2\pi\sum_{k<k_c}\frac{\langle\hat{n}_{\mathbf{k}}\rangle_0\langle\hat{n}_{-\mathbf{k}}\rangle_0}{k^2} \ .\end{aligned} \tag{4.5}$$

The first two lines are identical to the original Hamiltonian, Eq. (3.2), but with the small k (long wavelength) contributions to the electron-electron interactions omitted. The third line is the Hartree potential corresponding to those long wavelength Coulomb interactions,

$$\frac{1}{\sqrt{V}}\sum_i\sum_{k<k_c}\frac{4\pi\langle\hat{n}_{\mathbf{k}}\rangle_0}{k^2}e^{-i\mathbf{k}\cdot\hat{\mathbf{r}}_i} = \sum_i\int\frac{n^l(\mathbf{r}')}{|\hat{\mathbf{r}}_i - \mathbf{r}'|}d^3r' \ , \tag{4.6}$$

and the fourth line is the Hartree energy, which is subtracted to prevent double counting.

The short-range Hamiltonian is therefore equivalent to the original Hamiltonian, Eq. (3.2), but with the long wavelength parts of the Coulomb interaction treated within the Hartree approximation. Since the long wavelength parts of the effective potentials used in Hartree-Fock and LDA calculations are both dominated by the Hartree contributions, we might equally well say that $\hat{H}_{sr}$ is equivalent to the original Hamiltonian but with the small k Coulomb interactions approximated using Hartree-Fock or LDA (provided the HF or LDA density is sufficiently similar to the exact ground-state density).

In practice, of course, we do not attempt to solve $\hat{H}_{sr}$ exactly, but treat it within an independent electron approach such as Hartree-Fock or LDA. This additional approximation replaces the short-range part of the electron-electron interaction by a mean field, which simply adds

to the long wavelength mean field already introduced by the RPA. The overall effect is equivalent to starting from the original Hamiltonian and replacing the *full* interaction by a mean field. This implies that one can obtain the short-range "electronic" part of the RPA wave function by starting from the original fully interacting Hamiltonian and treating it using any sensible mean-field approximation. The best single-particle orbitals to use in the Slater determinant are therefore very close to the familiar Hartree-Fock or LDA orbitals; they are not significantly altered by the presence of the RPA plasmon wave function Ψ_p.

The short-range Hamiltonian of Eq. (4.5) still contains the full Coulomb interaction for $k > k_c$, and so still diverges like $1/r_{ij}$ whenever two electrons approach each other. The electron-electron cusps should therefore appear in the short-range electronic wave function, not in the wave function that describes the plasmons. One drawback of treating the short-range Hamiltonian within a mean-field approximation is that this neglects the electron-electron cusps, which play an important role in reducing the total energy of the many-electron system. This limitation of the mean-field treatment of $\hat{H}_{sr}$ may be remedied by building the cusps into Ψ_p instead.

B. Inverting the unitary transformation

The ground state of $\hat{H}_{\rm RPA}$ is the product of the ground states of $\hat{H}_{sr}$ and $\hat{H}_p$, neither of which commutes with the transformed subsidiary condition, Eq. (3.27). This implies that, unlike the ground state of $\hat{H}_{\rm BP}^{\rm new}$, the ground state of $\hat{H}_{\rm RPA}$ need not obey the subsidiary condition automatically. In consequence, the approximate ground state of $\hat{H}_{\rm BP}$ obtained by applying the back transformation, $\hat{S}^\dagger$, to the ground state of $\hat{H}_{\rm RPA}$, need not be an eigenfunction of the plasmon momentum operators, and we can no longer extract an approximation to the spatial ground state by simply forgetting about the $|\boldsymbol{\pi}\rangle$ factor in a product wave function of the form $|\psi\rangle|\boldsymbol{\pi}\rangle$. Fortunately, however, the subsidiary condition is still exact, and so still defines the subspace of the extended Hilbert space in which the true ground state lies. We can therefore take the ground state of the approximate Hamiltonian, $\hat{H}_{\rm RPA}$, and project it onto that subspace. The required projection operator to be applied after the back transformation is

$$\prod_{k<k_c} \left|\pi_{\mathbf{k}} = \pi_{\mathbf{k}}^0\right\rangle\left\langle\pi_{\mathbf{k}} = \pi_{\mathbf{k}}^0\right| \ . \tag{4.7}$$

As discussed in Sec. IV A, we approximate the ground state of $\hat{H}_{sr}$ as a Slater determinant D. The approximate ground state of the full Hamiltonian $\hat{H}_{\rm RPA}$ is therefore $\Phi_{\rm RPA}(\{\mathbf{r}_i\},\{\pi_{\mathbf{k}}\}) = \langle\{\mathbf{r}_i\},\{\pi_{\mathbf{k}}\}|\Phi_{\rm RPA}\rangle = \Psi_p(\{\pi_{\mathbf{k}}\})D(\{\mathbf{r}_i\})$. We can now obtain an approximate ground state of the original Hamiltonian $\hat{H}_{\rm BP}$ by back transforming using the inverse of the unitary transformation. The only important effect of the back transformation is to shift the numbers $\pi_{\mathbf{k}}$ appearing in Ψ_p as follows:

$$\pi_{\mathbf{k}} \to \pi_{\mathbf{k}} - \left(4\pi/k^2\right)^{1/2} n_{\mathbf{k}} \ , \tag{4.8}$$

where $n_{\mathbf{k}} = V^{-1/2}\sum_i e^{i\mathbf{k}\cdot\mathbf{r}_i}$. This can be verified by observing that, when evaluating a back-transformed wave function $\Phi^{\rm old}(\{\mathbf{r}_i\},\{\pi_{\mathbf{k}}\}) = \langle\{\mathbf{r}_i\},\{\pi_{\mathbf{k}}\}|\hat{S}^\dagger|\Phi\rangle$, we can apply the transformation to the bra $\langle\{\mathbf{r}_i\},\{\pi_{\mathbf{k}}\}|$ rather than the ket $|\Phi\rangle$. But since

$$\begin{aligned}
&\hat{\pi}_{\mathbf{k}}\hat{S}\left|\{\mathbf{r}_i\},\{\pi_{\mathbf{k}}\}\right\rangle = \hat{S}\hat{S}^\dagger\hat{\pi}_{\mathbf{k}}\hat{S}\left|\{\mathbf{r}_i\},\{\pi_{\mathbf{k}}\}\right\rangle \\
&= \hat{S}\left(\hat{\pi}_{\mathbf{k}} - \left(4\pi/k^2\right)^{1/2}\hat{n}_{\mathbf{k}}\right)\left|\{\mathbf{r}_i\},\{\pi_{\mathbf{k}}\}\right\rangle \\
&= \left(\pi_{\mathbf{k}} - \left(4\pi/k^2\right)^{1/2} n_{\mathbf{k}}\right)\hat{S}\left|\{\mathbf{r}_i\},\{\pi_{\mathbf{k}}\}\right\rangle \ ,
\end{aligned} \tag{4.9}$$

we see that

$$\hat{S}\left|\{\mathbf{r}_i\},\{\pi_{\mathbf{k}}\}\right\rangle = \left|\{\mathbf{r}_i\},\{\pi_{\mathbf{k}} - \left(4\pi/k^2\right)^{1/2} n_{\mathbf{k}}\}\right\rangle \ . \tag{4.10}$$

The $\pi_{\mathbf{k}}$ eigenvalues of the transformed bra are therefore shifted by $-\left(4\pi/k^2\right)^{1/2} n_{\mathbf{k}}$ relative to those of the original bra. As a result, $\Phi^{\rm old}(\{\mathbf{r}_i\},\{\pi_{\mathbf{k}}\}) = \Phi(\{\mathbf{r}_i\},\{\pi_{\mathbf{k}} - \left(4\pi/k^2\right)^{1/2} n_{\mathbf{k}}\})$.

Applying the projection operator given in Eq. (4.7) replaces the remaining $\pi_{\mathbf{k}}$ by $\pi_{\mathbf{k}}^0 = (4\pi/k^2)^{1/2}\langle\hat{n}_{\mathbf{k}}\rangle_0$. (In the homogeneous case this is zero.) All in all, then, the spatial part of the approximation to the ground state is

$$\Psi = \Psi_J D = \exp\left[\frac{1}{2}\sum_{i,j}\tilde{u}(\mathbf{r}_i,\mathbf{r}_j)\right] D \ , \tag{4.11}$$

where

$$\begin{aligned}
\tilde{u}(\mathbf{r},\mathbf{r}') = -4\pi \sum_{k,k'<k_c} \Bigg[\\
\left(\frac{e^{-i\mathbf{k}\cdot\mathbf{r}}}{\sqrt{V}} - \frac{\langle\hat{n}_{-\mathbf{k}}\rangle_0}{N}\right)\frac{\left[M^{-\frac{1}{2}}\right]_{\mathbf{k},\mathbf{k}'}}{kk'}\left(\frac{e^{i\mathbf{k}'\cdot\mathbf{r}'}}{\sqrt{V}} - \frac{\langle\hat{n}_{\mathbf{k}'}\rangle_0}{N}\right)\Bigg] .
\end{aligned} \tag{4.12}$$

The RPA Jastrow factor includes constant terms, one-electron terms, and two-electron terms. The constant terms may be ignored as they only affect the normalization of the wave function. The remaining one- and two-electron terms may then be disentangled and Ψ_J rewritten in the form,

$$\Psi_J = \exp\left[\frac{1}{2}\sum_{i,j}u(\mathbf{r}_i,\mathbf{r}_j) + \sum_i \chi(\mathbf{r}_i)\right] \ , \tag{4.13}$$

where $u(\mathbf{r},\mathbf{r}')$ and $\chi(\mathbf{r})$ are defined via:

$$u(\mathbf{r},\mathbf{r}') = -\frac{1}{V}\sum_{k,k'<k_c} e^{-i\mathbf{k}\cdot\mathbf{r}}\frac{4\pi\left[M^{-1/2}\right]_{\mathbf{k},\mathbf{k}'}}{kk'}e^{i\mathbf{k}'\cdot\mathbf{r}'}, \quad (4.14)$$

and

$$\chi(\mathbf{r}) = \frac{1}{\sqrt{V}}\sum_{k,k'<k_c} e^{-i\mathbf{k}\cdot\mathbf{r}}\frac{4\pi\left[M^{-1/2}\right]_{\mathbf{k},\mathbf{k}'}}{kk'}\langle\hat{n}_{\mathbf{k}'}\rangle_0 \quad (4.15)$$

$$= -\int_V u(\mathbf{r},\mathbf{r}')n^l(\mathbf{r}')d^3r' \; . \quad (4.16)$$

As in Eq. (3.20), $n^l(\mathbf{r})$ is the long wavelength $k < k_c$ part of the ground-state electron density. In k-space, the relationship between u and χ takes the form,

$$\chi(\mathbf{k}) = -\sum_{k'<k_c} u(\mathbf{k},\mathbf{k}')n(\mathbf{k}') \; , \quad (4.17)$$

discussed in Sec. II B.

In a homogeneous system, Eq. (4.3) reduces to $M_{\mathbf{k},\mathbf{k}'} = \omega_p^2\delta_{\mathbf{k},\mathbf{k}'}$. The χ function therefore vanishes and the u function becomes

$$u^{\rm hom}(\mathbf{k},\mathbf{k}') = -\frac{4\pi}{\omega_p}\frac{1}{kk'}\delta_{\mathbf{k},\mathbf{k}'} \; . \quad (4.18)$$

Transforming to real space we obtain

$$\begin{aligned} u^{\rm hom}(\mathbf{r},\mathbf{r}') &= u^{\rm hom}(|\mathbf{r}-\mathbf{r}'|) \\ &= -\frac{1}{V}\frac{1}{\omega_p}\sum_{k<k_c} e^{-i\mathbf{k}\cdot(\mathbf{r}-\mathbf{r}')}\frac{4\pi}{k^2} \; . \end{aligned} \quad (4.19)$$

If k_c is set equal to infinity this gives

$$u^{\rm hom}(|\mathbf{r}-\mathbf{r}'|) = -\frac{1}{\omega_p|\mathbf{r}-\mathbf{r}'|} \; . \quad (4.20)$$

For finite k_c, the divergence of $u(|\mathbf{r}-\mathbf{r}'|)$ at small $|\mathbf{r}-\mathbf{r}'|$ is suppressed, but the $1/|\mathbf{r}-\mathbf{r}'|$ decay at large $|\mathbf{r}-\mathbf{r}'|$ remains more or less unaltered.

C. The cusp conditions in inhomogeneous systems

Sec. II A explained how cusps may be built in to a homogeneous RPA Jastrow factor by adding an exponential factor to the u function:

$$u(r) = -\frac{1}{\omega_p r}\left(1 - e^{-r/F}\right) \; . \quad (4.21)$$

At large r this u function has the $1/(\omega_p r)$ behavior implied by the RPA, while at small r it tends smoothly towards the required cusp at $r = 0$. When supplemented by appropriate χ functions, such Jastrow factors are remarkably successful. It is therefore worth considering how we might add cusps to our inhomogeneous RPA u function.

This is not easy, since the inhomogeneous u function is given as a complicated truncated double Fourier series. The series determines the behavior of $u(\mathbf{r},\mathbf{r}')$ when $\mathbf{r}-\mathbf{r}'$ is large, and we have to find a way of splicing this known long-range behavior onto the cusp which fixes the slope of $u(\mathbf{r},\mathbf{r}')$ as $|\mathbf{r}-\mathbf{r}'| \to 0$. It turns out that this interpolation problem is easiest to handle when expressed in k-space.

Eq. (4.21) can be Fourier analyzed to give:

$$u(\mathbf{k}) = \frac{-4\pi}{\sqrt{V}\omega_p}\frac{1/F^2}{k^2(k^2+1/F^2)} \; . \quad (4.22)$$

Using the cusp conditions, Eq. (2.3), we see that $1/F^2 = C\omega_p$, where $C = 1$ for antiparallel spins and $C = 1/2$ for parallel spins. Hence

$$u(\mathbf{k}) = \frac{-4\pi}{\sqrt{V}}\frac{C}{k^2(k^2+C\omega_p)} \; . \quad (4.23)$$

In Sec. V B we test a homogeneous u function defined using a truncated Fourier series of this form and find that most of the cusp energy can be retrieved using a reasonably low cutoff.

Eq. (4.23) defines a natural k-space crossover, k_x, given by $k_x^2 = C\omega_p$. The terms with $k < k_x$ produce the RPA behavior at large r, while for $k > k_x$ we have $u(\mathbf{k}) \propto 1/k^4$, which generates the cusp. The density dependence of k_x differs from that of the plasmon cutoff k_c from Eq. (3.1). It turns out, however, that for typical metallic densities k_c and k_x are both of the order of k_F. The $k^2 + C\omega_p$ factor in the denominator of Eq. (4.23) therefore allows us to introduce the cusp without significantly affecting the large r ($k < k_c$) behavior implied by the RPA. If the density is extremely small, k_x ($\propto \omega_p^{1/2} \propto n^{1/4}$) is smaller than k_c ($\propto n^{1/6}$), and so this method for imposing the cusp is no longer consistent with the RPA limit.

Eq. (4.23) suggests a simple k-space prescription for building a cusp into the inhomogeneous Jastrow factor. We write the inhomogeneous Jastrow factor as a double Fourier series,

$$u(\mathbf{r},\mathbf{r}') = \frac{1}{V}\sum_{\mathbf{k},\mathbf{k}'} e^{-i\mathbf{k}\cdot\mathbf{r}}u(\mathbf{k},\mathbf{k}')e^{i\mathbf{k}'\cdot\mathbf{r}'} \; , \quad (4.24)$$

noting that in a homogeneous system we have $u(\mathbf{k},\mathbf{k}') = \sqrt{V}u(\mathbf{k})\delta_{\mathbf{k},\mathbf{k}'}$. We use this relationship to rewrite the homogeneous u function of Eq. (4.23) in a form suitable for generalization to the inhomogeneous case,

$$u(\mathbf{k},\mathbf{k}') = -\frac{4\pi C}{kk'}\left(kk'\delta_{\mathbf{k},\mathbf{k}'} + C\omega_p\delta_{\mathbf{k},\mathbf{k}'}\right)^{-1} \; , \quad (4.25)$$

where the inversion is interpreted that of a (diagonal) matrix. In the absence of cusps, we have seen that the homogeneous Jastrow factor may be obtained from the inhomogeneous one by replacing

$$M_{\mathbf{k},\mathbf{k}'} = \frac{1}{V}\frac{(\mathbf{k}\cdot\mathbf{k}')}{kk'}\int e^{i(\mathbf{k}-\mathbf{k}')\cdot\mathbf{r}}\omega_p^2(\mathbf{r})d^3r \quad (4.26)$$

by $\omega_p^2\delta_{\mathbf{k},\mathbf{k}'}$. As we now wish to extrapolate from a homogeneous Jastrow factor to an inhomogeneous one, we do the opposite and replace $\omega_p\delta_{\mathbf{k},\mathbf{k}'} = (\omega_p^2\delta_{\mathbf{k},\mathbf{k}'})^{1/2}$ by the matrix square root $M^{1/2}_{\mathbf{k},\mathbf{k}'}$. Eq. (4.25) then becomes

$$\begin{aligned} u(\mathbf{k},\mathbf{k}') &= -\frac{4\pi C}{kk'}\left(kk'\delta_{\mathbf{k},\mathbf{k}'} + CM^{1/2}_{\mathbf{k},\mathbf{k}'}\right)^{-1} \\ &= -\frac{4\pi C}{(kk')^2}\left(\delta_{\mathbf{k},\mathbf{k}'} + \frac{CM^{1/2}_{\mathbf{k},\mathbf{k}'}}{kk'}\right)^{-1} . \end{aligned} \tag{4.27}$$

By expressing $M^{1/2}_{\mathbf{k},\mathbf{k}'}$ in terms of the original cuspless u function, Eq. (4.27) can be cast in a form that is applicable to a wide variety of cuspless correlation terms.

If we make the reasonable assumption that the Fourier series for $\omega_p^2(\mathbf{r})$ converges rapidly, the elements of the matrix M are constant along the diagonal and fall off as we move away from the diagonal. For large k and k' this guarantees that $u(\mathbf{k},\mathbf{k}')$ is dominated by the $1/(kk')^2 \approx 1/k^4$ prefactor, generating a cusp. For small k and k' we have

$$u(\mathbf{k},\mathbf{k}') \approx -\frac{4\pi C}{(kk')^2}\left(\frac{CM^{1/2}_{\mathbf{k},\mathbf{k}'}}{kk'}\right)^{-1} = -4\pi\frac{M^{-1/2}_{\mathbf{k},\mathbf{k}'}}{kk'} , \tag{4.28}$$

which is the RPA result. The u function of Eq. (4.27) therefore interpolates smoothly between the anisotropic long-range correlation term derived from the inhomogeneous RPA and the cusp at short range.

D. The one-body term

The introduction of the cusp modifies the $k < k_c$ Fourier components of the RPA u function and introduces nonzero Fourier components with $k > k_c$. In addition, it makes the u function spin dependent, suggesting that we need a spin-dependent one-body term. We therefore generalize our expression for $\chi(\mathbf{k})$ from Eq. (4.17) by extending the wave vector sum to include components with $k > k_c$ and introducing a sum over spin indices,

$$\chi_\uparrow(\mathbf{k}) = -\sum_{\mathbf{k}'}\left[u_{\uparrow\uparrow}(\mathbf{k},\mathbf{k}')n_\uparrow(\mathbf{k}') + u_{\uparrow\downarrow}(\mathbf{k},\mathbf{k}')n_\downarrow(\mathbf{k}')\right] , \tag{4.29}$$

with an equivalent formula for $\chi_\downarrow(\mathbf{k})$. In an unpolarized system, where $n_\uparrow(\mathbf{k}') = n_\downarrow(\mathbf{k}') = \frac{1}{2}n(\mathbf{k}')$, this reduces to

$$\chi_\uparrow(\mathbf{k}) = -\sum_{\mathbf{k}'}\frac{1}{2}\left[u_{\uparrow\uparrow}(\mathbf{k},\mathbf{k}') + u_{\uparrow\downarrow}(\mathbf{k},\mathbf{k}')\right]n(\mathbf{k}') . \tag{4.30}$$

In the case of a homogeneous correlation term u this further reduces to

$$\chi_\uparrow(\mathbf{k}) = -\frac{1}{2}\sqrt{V}\left[u_{\uparrow\uparrow}(\mathbf{k}) + u_{\uparrow\downarrow}(\mathbf{k})\right]n(\mathbf{k}) , \tag{4.31}$$

as first proposed by Malatesta *et al.*[13]

V. RESULTS

This section assesses the effectiveness and accuracy of QMC trial wave functions containing RPA Jastrow factors. Sec. V A describes the systems studied and explains how the results are presented; Sec. V B considers homogeneous systems; and Sec. V C looks at inhomogeneous systems.

All the results were obtained using trial wave functions of the standard Slater-Jastrow form, where the spin-up and spin-down Slater determinants were constructed using accurate LDA orbitals. The Jastrow factor contained two- and one-body terms, $u(\mathbf{r}_i,\mathbf{r}_j)$ and $\chi(\mathbf{r}_i)$, of various different types. Note that from now on we drop the $u(\mathbf{r}_i,\mathbf{r}_i)$ self-interaction terms from the Jastrow factor. This is equivalent to altering $\chi(\mathbf{r}_i)$ by a negligible amount (ca. 5%).

The Monte Carlo runs discussed in the rest of this section were accumulated using samples of 10,000 statistically independent configurations of all the electrons, except for the energy data for the inhomogeneous system discussed in Sec. V C, where we used 100,000 configurations. The quoted standard deviations characterize the fluctuations of the individual local energy readings; the errors in the mean energies are given in brackets.

A. System geometry

The Hamiltonian is chosen to obey periodic boundary conditions with a simulation cell consisting of the Wigner-Seitz cell of a face-centered cubic (FCC) lattice. The lattice vectors of the simulation-cell lattice will be denoted by $\mathbf{A}_1$, $\mathbf{A}_2$, and $\mathbf{A}_3$, and the corresponding body-centered cubic (BCC) reciprocal lattice vectors by $\mathbf{B}_1$, $\mathbf{B}_2$, and $\mathbf{B}_3$.

For reasons of simplicity, we have chosen to study electron gas systems subject to external potentials that vary along the $\mathbf{B}_3$ direction only,[26]

$$V_{\text{ext}}(\mathbf{r}) = V_0\cos(\mathbf{B}_3\cdot\mathbf{r}) , \tag{5.1}$$

where $V_0 = 1$ in atomic units. Since $\mathbf{B}_3$ is a reciprocal lattice vector, this choice ensures that the potential has the same periodicity as the simulation cell. The electron density and χ functions, which also vary only in the $\mathbf{B}_3$ direction, share this periodicity.

The two-body term must also respect the periodic boundary conditions applied to the simulation cell. This implies that analytic Jastrow factors based on the u function of Eq. (4.21) must be made periodic by including contributions from all the electrons in a periodic lattice of identical copies of the simulation cell. Since the analytic u function decays like $1/r$ at large r, the sum of contributions is evaluated using Ewald summation techniques. Numerical Jastrow factors calculated from the inhomogeneous RPA are periodic by construction.

The next two subsections contain a number of figures showing electron densities, χ functions, and u functions. Charge densities and χ functions are plotted along the $\mathbf{B}_3$ direction from one side of the simulation cell to the other. The inhomogeneous two-body term $u(\mathbf{r}_1, \mathbf{r}_2)$ is more difficult to represent. We have chosen to fix the position $\mathbf{r}_1$ of the first electron, while sweeping $\mathbf{r}_2$ along the $\mathbf{B}_3$ direction on a line passing through $\mathbf{r}_1$. Fig. 1 shows the three positions of the first electron considered.

B. Homogeneous systems

The FCC simulation cell considered in this section held an unpolarized uniform electron gas of 61 up-spin electrons and 61 down-spin electrons. The density parameter r_s was equal to 2, corresponding to a Fermi wave vector k_F=$0.96a_0^{-1}$. Two different Jastrow factors were considered:

a. Homogeneous RPA without cusps. The homogeneous RPA theory suggests using a correlation term of the form,

$$u(\mathbf{r}_i, \mathbf{r}_j) = \frac{-4\pi}{V\omega_p} \sum_{k<k_c} \frac{1}{k^2} e^{i\mathbf{k}\cdot(\mathbf{r}_i - \mathbf{r}_j)} \; . \tag{5.2}$$

We saw in the introduction to Sec. III that for typical metallic densities the cutoff k_c is comparable to the Fermi wave vector k_F.

b. Homogeneous RPA with cusps. In Sec. II A we saw how a cusp may be introduced by adding an exponential factor to the $k_c \to \infty$ limit of the homogeneous RPA u function,

$$u_{\sigma_i\sigma_j}(r_{ij}) = -\frac{1}{\omega_p r_{ij}} (1 - e^{-r_{ij}/F_{\sigma_i\sigma_j}}) \; , \tag{5.3}$$

where $F_{\sigma_i\sigma_j}$ is chosen appropriately.

Table I shows the local energy averages and standard deviations obtained in VQMC simulations using these two Jastrow factors. For comparison, we also show results obtained using a "Hartree-Fock" trial function including up- and down-spin Slater determinants of LDA orbitals (in this case plane waves) but no Jastrow factor. The introduction of an RPA Jastrow factor without a cusp lowers the calculated energy considerably but has little effect on the standard deviation. The introduction of the cusp lowers the energy greatly and also reduces the standard deviation. It is clear that the presence of the cusp is vital if accurate total energies are to be obtained.

In Eq. (4.23) we saw how the u function with a cusp from Eq. (5.3) may be represented as a Fourier series. We can investigate the usefulness of this representation by cutting off the series at a wave vector k_n and varying k_n to see how fast the calculated VQMC energy converges. Fig. 2 shows the convergence of the energy graphically. It can be seen that a cutoff of k_n=$3.95a_0^{-1}$ produces a wave function with the same energy (to within statistical uncertainties) as an infinite cutoff. As the $3.95a_0^{-1}$ cutoff is small enough to be computationally feasible, there is no difficulty in representing the cusp in k-space. Note also how the standard deviation decreases as the energy improves.

C. Inhomogeneous systems

As mentioned above, the inhomogeneous systems we consider have a background potential that varies in one dimension only. The strongly inhomogeneous LDA electron density of the unpolarized 64 electron simulation cell considered in this subsection is shown in Fig. 3. The average electron density is the same as that of a uniform system with r_s=2 and Fermi wave vector k_F^0=$0.96a_0^{-1}$. The LDA result for the energy is -15.658×10^{-2} eV per electron.

In addition to investigating the influence of the cusp, as in the homogeneous case, we must also now investigate the effects of the one-body χ function and compare the accuracies of homogeneous and inhomogeneous u functions. We therefore split this section into three subsections:

1. First we look at the pure (i.e. cuspless) homogeneous RPA Jastrow factor (which has no χ function) and compare it with the pure inhomogeneous RPA Jastrow factor (which does have a χ function).

2. Second we investigate the effects of adding cusps to these two correlation factors.

3. Finally we add an ad-hoc one-body χ term to the homogeneous RPA Jastrow factor.

1. Inhomogeneous RPA without cusps

The inhomogeneous RPA Jastrow factor considered here is the one derived in Sec. IV A (Eqs. (4.13), (4.14), and (4.15)), which includes both u and χ functions. As always in this work, the matrix M is constructed using the LDA density, and the Slater determinants contain LDA orbitals. The homogeneous RPA Jastrow factor includes the u function from Eq. (5.2) but no χ. In both cases the cutoff k_c is set equal to the Fermi wave vector, k_F^0=$0.96a_0^{-1}$, of a homogeneous system with the same average electron density as the inhomogeneous system.

Table II compares the VQMC energies and standard deviations calculated using the homogeneous (RPA1) and inhomogeneous (RPA2) Jastrow factors without cusps. It is clear that the inhomogeneous Jastrow factor is much the better of the two. The reason is apparent from Fig. 3, which demonstrates that the inhomogeneous Jastrow factor, which has a built-in one-body term, produces a near optimal density. Fig. 3 also shows that the homogeneous RPA Jastrow factor (which has no one-body term) gives

a very poor electron density. This explains why the corresponding VQMC energy is so poor

In Fig. 4 we plot the inhomogeneous RPA two-body term. Both inhomogeneity and anisotropy can be seen. To aid understanding, Fig. 5 shows the Jastrow factors of three different homogeneous systems, the constant densities of which correspond to the *local* densities at the central positions of plots A, B, and C, respectively. It is clear that the three inhomogeneous u functions shown in Fig. 4 are much more similar than the three homogeneous u functions shown in Fig. 5. This shows that the inhomogeneous RPA u function is not well approximated by a local-density-like approximation based on the homogeneous RPA.[27]

At point B, the charge density around the electron is asymmetric, and this is reflected in the anisotropy of the u function. We find that the Jastrow factor has a larger range in the low density regions than in the high density regions, consistent with the "local density" picture of Fig. 4 and with the physical expectation that screening should be more effective at high densities. This interpretation also explains the shape of the anisotropy: the u function is weaker on the high density side where the screening is more effective. We find, however, that the range of variation of the inhomogeneous Jastrow factor is much smaller than predicted by the "local density" picture.

2. Inhomogeneous RPA with cusps

A cusp may be added to the inhomogeneous RPA u function using the Fourier-space method explained in Sec. IV C. The results discussed below are obtained with a Fourier cutoff k_n of $4.95a_0^{-1}$; Fig. 2 suggests that this is large enough to represent the cusp accurately. Since we choose not to change the relationship between the u and χ functions, Eq. (2.9), the introduction of the cusp also modifies the one-body χ function.

The addition of the cusp to the inhomogeneous RPA Jastrow factor (to produce the Jastrow factor denoted RPA3 in Table II) reduces the calculated VQMC energy from $-13.32(1) \times 10^{-2}$ eV per electron to $-15.795(4) \times 10^{-2}$ eV per electron. The latter is the best variational estimate of the energy we were able to obtain using any of the Jastrow factors considered in this paper. The addition of cusps to the homogeneous u function does not introduce a one-body term and so the density obtained using the homogeneous RPA Jastrow factor is still poor. Energies calculated using the homogeneous RPA Jastrow factor therefore remain much worse than energies calculated using the inhomogeneous RPA Jastrow factor.

Fig. 6, which is analogous to Fig. 4, shows the inhomogeneous RPA u function after the cusp has been added. It is clear that the addition of the cusp greatly reduces the amount of inhomogeneity and anisotropy. Despite the fact that the system is strongly inhomogeneous, the cusp acts as such a stringent constraint that $u(\mathbf{r}_i, \mathbf{r}_j)$ is close to homogeneous. Although the inhomogeneity derived from the RPA must persist when $|\mathbf{r}_i - \mathbf{r}_j|$ is large enough, the crossover length, $2\pi/k_x$, corresponding to the average density r_s=2, is comparable to our system size. This implies that the form of the u function is largely determined by the cusp throughout our system. If we had studied larger systems we would have seen the RPA reassert itself at large $|\mathbf{r}_i - \mathbf{r}_j|$, but previous work on numerical trial function optimization[28] and finite-size errors[29,30] has shown that the behavior of the u function at such large values of $|\mathbf{r}_i - \mathbf{r}_j|$ has very little effect on the total energy. The fact that the inhomogeneous u function becomes so homogeneous once the cusp has been added explains the surprisingly good performance of the homogeneous u functions used in most QMC simulations of solids.

3. Variance optimized one- and two-body terms

In this subsection we compare Jastrow factors based on the inhomogeneous RPA theory with Jastrow factors obtained using numerical variance optimization.

We have already explained that we always construct the χ function appearing in the inhomogeneous RPA Jastrow factor from the u function and density according to Eq. (2.9). Although Eq. (2.9) was derived within the RPA, we assume that it holds unaltered even after the spin-dependent cusps have been added to u. This assumption proves very successful in practice, yielding χ functions that are not significantly worse than those computed (at much greater cost) using numerical variance optimization.

When adding a χ function to the homogeneous u function of Eq. (5.3) we have two options: we could try using Eq. (2.9) again, or we could use variance minimization. Since u is now a function of $|\mathbf{r}_i - \mathbf{r}_j|$ only, Eq. (2.9) reduces to Eq. (2.10), which was first derived by Malatesta *et al.*[13,14] The impressive accuracy of Eq. (2.10) is shown in Fig. 7, where we compare the analytic χ function with one obtained using additional numerical variance optimization. We see that the two χ functions (and hence the two electron densities) are very similar. The corresponding change in the energy (denoted VM1 in Table II) is not statistically significant.

In addition, in Table II, we give the energy (denoted VM2) calculated using numerically optimized (homogeneous) u and χ functions of the type described by Williamson *et al.*[28] It may appear surprising that this very general optimization procedure yields such disappointing results, but the explanation is simple: for computational reasons, the variance optimized u function is constrained to be zero everywhere on the cell boundary, and this is a significant drawback in small simulation cells such as ours. In larger simulation cells the behaviour of the u function at the cell boundary is less important and

the optimized u function outperforms the familiar Ewald form.

A comparison (see Table II) of the results for the RPA3 Jastrow factor, which has an inhomogeneous u function with a cusp, and the RPA4 Jastrow factor, which has a homogeneous u function with a cusp, shows that the inhomogeneity of the u function provides a small but significant improvement. The energy difference amounts to 3.3 standard deviations, and so the probability that it is negative (i.e., that the introduction of inhomogeneity is actually an improvement) is 99.96%.

The effect of the finite cutoff k_n can also be seen in Table II, by comparing the RPA4 result with the result for the Ewald-summed Jastrow factor (EW). Note that both of these Jastrow factors have a cusp and include the same χ function from Eq. (2.10). Furthermore, as $k_n \to \infty$, the two Jastrow factors become identical and the RPA4 result tends to the EW result. We see that the presence of the exact cusp in the EW Jastrow factor reduces the variance slightly but provides a statistically insignificant improvement in the energy. Since both these Jastrow factors include homogeneous u functions, neither is as good as the inhomogeneous Jastrow function RPA3. As far as the energy is concerned, we conclude that despite the dominance of the cusp and the one-body term, the inhomogeneity of the RPA correlations does produce a small but measurable improvement.

The small size of the improvement due to the inhomogeneity of the u function is consistent with previous work and may be explained as follows. In the system considered here the LDA, which is based on a very simple spherical approximation to the exchange-correlation hole, yields a very accurate energy of -15.658×10^{-2} eV per electron. Because this result is so good, any benefits to be gained by improving the description of the hole must necessarily be fairly small. The difference between the LDA and homogeneous VMC energies is about 0.12×10^{-2} eV per electron, and the introduction of the inhomogeneous u function yields another 0.02×10^{-2} eV per electron; the effect of the inhomogeneity is therefore a substantial 15% of the difference between the VMC and LDA energies.

VI. COMPUTATIONAL EFFICIENCY

The inhomogeneous Jastrow factor consists of a double Fourier sum and a sum over all the electrons. By rearranging these sums the computational effort can be made to scale as N_e^2 for each single electron move, where N_e is the number of electrons. In contrast, the scaling of QMC simulations using homogeneous Jastrow factors is $N_e + \epsilon N_e^2$, where ϵ is often fairly small.[9] The introduction of the inhomogeneous u function is certainly not without computational cost, but does not affect the asymptotic scaling of the QMC algorithm.

As we were interested in evaluating the quality of the trial function rather than in computational efficiency, we did not optimize our programs for speed. Nevertheless, the generation of 100,000 configurations for the 64 electron system takes only a couple of days on a modern workstation. Furthermore, as the time required to evaluate the inhomogeneous Jastrow factor scales as the sixth power of the Fourier cutoff k_n, the speed of the calculation could be dramatically improved by reducing k_n. Our chosen cutoff of $4.95 a_0^{-1}$ was very conservative, and the small errors introduced by reducing it could easily be corrected. Using a sensible choice for k_n and optimized code running on a workstation, the inhomogeneous RPA Jastrow factor could certainly be used to study comparably-sized simulation cells of real (pseudo)solid.

In fact, the overwhelming majority of the effort involved in a typical solid state VMC calculation concerns the generation and optimization of trial functions. The greatest advantage of the RPA-based approach discussed in this paper is that it provides accurate analytic u and χ functions, thus avoiding or dramatically reducing the need for numerical wavefunction optimization.

VII. CONCLUSIONS

Our principal aim was to better understand the physics underlying the Slater-Jastrow trial wave functions used in QMC simulations of solids. We began by generalizing Bohm and Pines' RPA treatment of the homogeneous electron gas[11] to the inhomogeneous case. The result of this analysis was a Slater-Jastrow trial wave function containing an anisotropic inhomogeneous Jastrow factor expressed as a double Fourier sum. The optimal orbitals appearing in the Slater determinants were shown to be close to Hartree-Fock or LDA orbitals, even though these theories do not include Jastrow factors.

The RPA describes the long-range electronic correlations accurately, but not the scattering-like correlations at short distances. We saw, however, that the correct short-range behavior determined by the cusp conditions may easily be imposed on any Jastrow factor represented in k-space. When the inhomogeneous RPA result is modified in this way, the result is a parameter-free Jastrow factor with the correct short and long-range behavior. Unlike previous work,[13,14] this approach provides both u and χ functions, not just a relationship between them.

For a system of 64 electrons in a strong sinusoidal external potential, we showed that trial functions incorporating modified RPA Jastrow factors are both accurate and computationally tractable. Since such Jastrow factors are parameter-free, the time-consuming variance minimization procedure normally used to generate accurate χ functions is not required. The inhomogeneity of the two-body u function yields only a small benefit in the system we studied, but even this small improvement is $\sim$15% of the difference between the LDA and homogeneous VMC energies. The reason why these differences

are not larger, and the reason why homogeneous u functions often work so well, is that the imposition of the cusp conditions washes out most of the inhomogeneity of the RPA u function when $|\mathbf{r}_i - \mathbf{r}_j|$ is small.

If we compare the plasmon cutoff k_c ($\propto n^{1/6}$) from Eq. (3.1) with the wave vector k_x ($\propto n^{1/4}$) that characterizes the crossover from screening behavior to cusplike behavior (see Sec. IV C), we see that the cusp is relatively less important in high density systems. This suggests that the inhomogeneity of the RPA u function may produce a more obvious improvement when the average electron density is both large and strongly varying. This is intuitively sensible, since in low density systems we expect the short-range electron-electron scattering described by the cusp to dominate, whereas at higher densities screening and collective effects should be more important. Possible candidates for high density systems include calculations explicitly involving the core electrons, where it is already known that the use of inhomogeneous u functions is advantageous.[22] Other systems where one might expect inhomogeneities in the correlation term to become important are rare earth elements, where some of the valence electrons are strongly bound to the core.

---

* Present address: Department of Chemistry, Queen Mary and Westfield College, Mile End Road, London E1 4NS, UK.

[1] M. H. Kalos and P. A. Whitlock, *Monte Carlo Methods Volume 1: Basics* (Wiley, New York, 1986).
[2] B. L. Hammond, W. A. Lester, Jr., and P. J. Reynolds, *Monte Carlo Methods in Ab Initio Quantum Chemistry* (World Scientific, Singapore, 1994).
[3] S. Fahy, X. W. Wang, and S. G. Louie, Phys. Rev. Lett. **61**, 1631 (1988).
[4] S. Fahy, X. W. Wang, and S. G. Louie, Phys. Rev. B **42**, 3503 (1990).
[5] X.–P. Li, D. M. Ceperley, and R. M. Martin, Phys. Rev. B **44**, 10929 (1991).
[6] G. Rajagopal, R. J. Needs, A. James, S. D. Kenny, and W. M. C. Foulkes, Phys. Rev. B **51**, 10591 (1995).
[7] P. R. C. Kent, R. Q. Hood, A. J. Williamson, R. J. Needs, W. M. C. Foulkes, and G. Rajagopal, Phys. Rev. B **59**, 1917 (1999).
[8] R. G. Parr and W. Yang, *Density Functional Theory of Atoms and Molecules* (Oxford University, New York, 1989).
[9] W. M. C. Foulkes, L. Mitas, R. J. Needs and G. Rajagopal, accepted for publication in Rev. Mod. Phys. (2001).
[10] N. Metropolis, A. W. Rosenbluth, M. N. Rosenbluth, A. H. Teller, and E. Teller, J. Chem. Phys. **21**, 1087 (1953).
[11] D. Bohm and D. Pines, Phys. Rev. **92**, 609 (1953).
[12] D. M. Ceperley, Phys. Rev. B **18**, 3126 (1978).
[13] A. Malatesta, S. Fahy, and G. B. Bachelet, Phys. Rev. B **56**, 12201 (1997).
[14] S. Fahy, in *Quantum Monte Carlo Methods in Physics and Chemistry*, Nato Science Series C: Mathematical and Physical Sciences, Vol. 525, edited by M. P. Nightingale and C. J. Umrigar (Kluwer Academic, Dordrecht, The Netherlands, 1999), p. 101.
[15] K. E. Schmidt and J. W. Moskowitz, J. Chem. Phys. **97**, 3382 (1992).
[16] C.–J. Huang, C. J. Umrigar, and M. P. Nightingale, J. Chem. Phys. **107**, 3007 (1997).
[17] W. M. C. Foulkes, R. Q. Hood, and R. J. Needs, Phys. Rev. B **60**, 4558 (1999).
[18] T. Kato, Communications on Pure and Applied Mathematics **10**, 151 (1957).
[19] R. T. Pack and W. B. Brown, J. Chem. Phys. **45**, 556 (1966).
[20] T. Gaskell, Proc. Phys. Soc. **77**, 1182 (1961); Proc. Phys. Soc. **80**, 1091 (1962).
[21] E. Krotscheck, W. Kohn, and G. X. Qian, Phys. Rev. B **32**, 5693 (1985).
[22] C. J. Umrigar, K. G. Wilson, and J. W. Wilkins, Phys. Rev. Lett. **60**, 1719 (1988).
[23] P. R. C. Kent, R. J. Needs, and G. Rajagopal, Phys. Rev. B **59**, 12344 (1999).
[24] D. Bohm, K. Huang, and D. Pines, Phys. Rev. **107**, 71 (1957).
[25] S. Raimes, *Many-Electron Theory* (North-Holland, Amsterdam-London, 1972).
[26] M. Nekovee, W. M. C. Foulkes, A. J. Williamson, G. Rajagopal, and R. J. Needs, Adv. Quantum Chem. **33**, 189 (1999).
[27] H. J. Flad, A. Savin, J. Chem. Phys. **103**, 691 (1995).
[28] A. J. Williamson, S. D. Kenny, G. Rajagopal, A. J. James, R. J. Needs, L. M. Fraser, W. M. C. Foulkes, and P. Maccallum, Phys. Rev. B **53**, 9640 (1996).
[29] L. M. Fraser, W. M. C. Foulkes, G. Rajagopal, R. J. Needs, S. D. Kenny, and A. J. Williamson, Phys. Rev. B **53**, 1814 (1996).
[30] A. J. Williamson, G. Rajagopal, R. J. Needs, L. M. Fraser, W. M. C. Foulkes, Y. Wang, and M.-Y. Chou, Phys. Rev. B **55**, R4851 (1997).

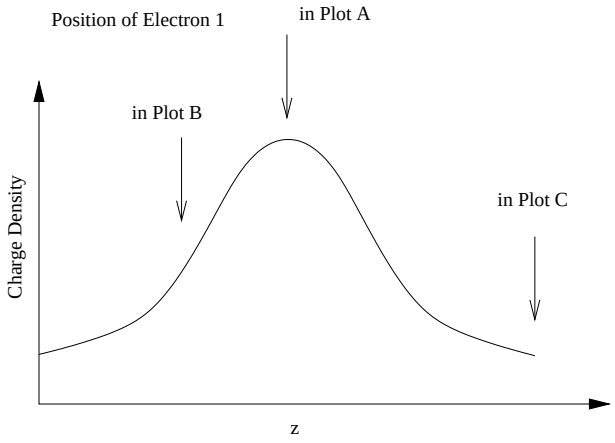

FIG. 1. In figures showing two-body terms, plots labeled A, B and C respectively show $u(\mathbf{r}_1, \mathbf{r}_2)$ as a function of $\mathbf{r}_2$ for $\mathbf{r}_1$ fixed at the peak (A), the average (B), and the minimum (C) of the electron density. In all cases $\mathbf{r}_2$ is swept along the $\mathbf{B}_3$ direction on a line passing through $\mathbf{r}_1$. The relative coordinate z measures the distance between the two electrons and thus equals zero when the two electrons are at the same place, irrespective of the fixed position of $\mathbf{r}_1$.

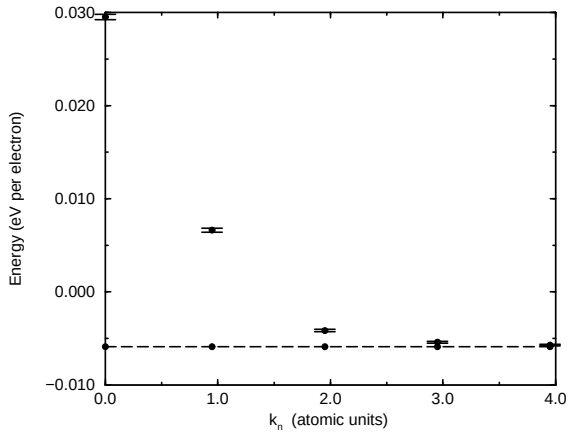

FIG. 2. The convergence of the VQMC energy as a function of the cutoff k_n used in the truncated Fourier series representation of the u function from Eq. (5.3). The results are for the uniform system considered in Sec. V B. The dotted line shows the calculated value of the energy when k_n=∞ (the standard deviation of this result is too small to show here).

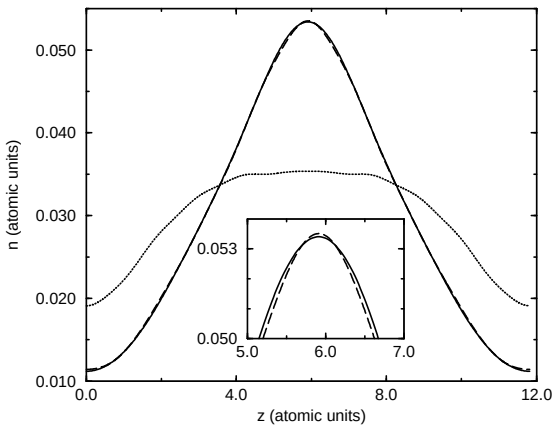

FIG. 3. The electron density of the strongly inhomogeneous 64 electron system considered in Sec. V C. The LDA density (solid line) is compared to the densities obtained using the homogeneous RPA (dotted line) and the inhomogeneous RPA (dashed line); the z-axis lies along the $\mathbf{B}_3$ direction.

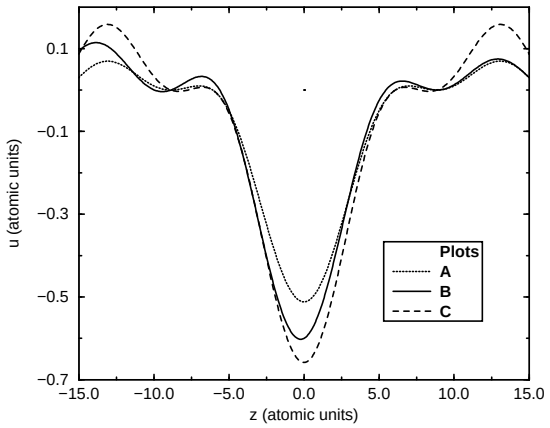

FIG. 4. The inhomogeneous RPA u function with no cusp for three different positions of the fixed electron. The results are for the inhomogeneous system considered in Sec. V C. The definition of z and the positions of A, B, and C are explained in Fig. 1. The Jastrow factor is stronger in the low density region.

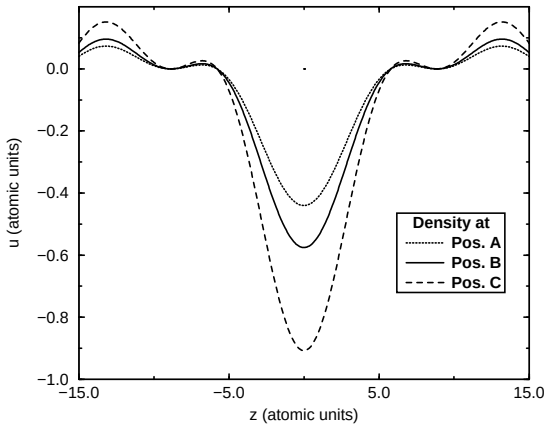

FIG. 5. The RPA u functions for three different uniform electron gases, the densities of which are equal to the densities at points A, B, and C of the strongly inhomogeneous 64 electron system considered in Sec. V C. The definition of z and the positions of A, B, and C are explained in Fig. 1. The homogeneous u functions are of course isotropic.

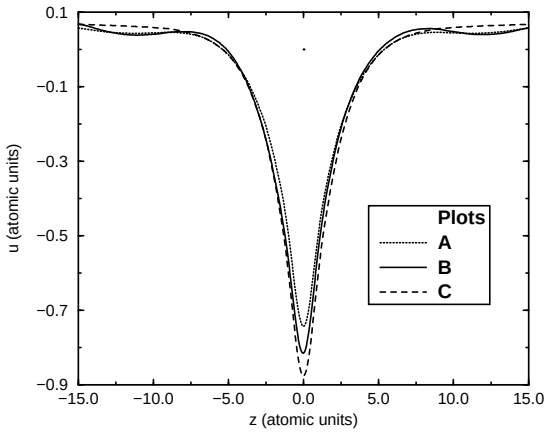

FIG. 6. The inhomogeneous RPA u function with a cusp for three different positions of the fixed electron. The results are for the strongly inhomogeneous 64 electron system considered in Sec. V C. The definition of z and the positions of A, B, and C are explained in Fig. 1. The addition of the cusp reduces the inhomogeneity and anisotropy observed in Fig. 4.

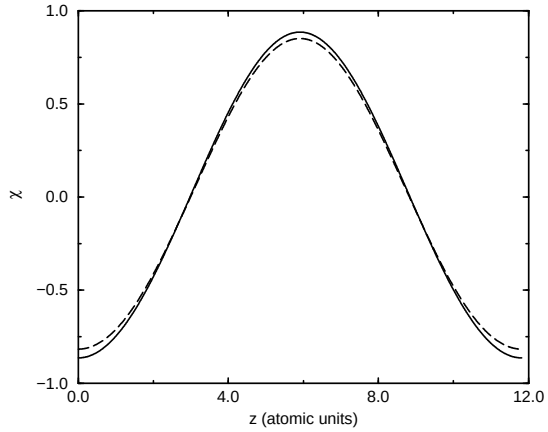

FIG. 7. Comparison of the χ function (solid line) obtained from Eq. (2.10) with one (dashed line) obtained using additional variance minimization. The results are for the strongly inhomogeneous 64 electron system considered in Sec. V C, using the homogeneous Ewald-summed Jastrow factor with cusp. The corresponding energies are equal to within the statistical error.

TABLE I. VQMC local energy averages E and standard deviations σ of the uniform system considered in Sec. V B in units of of 10^{-2}eV per electron. Results for three different trial wave functions are shown. The HF trial function has no Jastrow factor. The RPA results use the "pure" RPA u function from Eq. (5.2). The best energies are obtained using the RPA u function with a cusp from Eq. (5.3).

	HF	RPA	RPA+CUSP
E	2.951(28)	1.942(26)	-0.589(05)
σ	2.79	2.60	0.50

TABLE II. *VMC local energy averages E and standard deviations σ for the inhomogeneous system considered in Section V C. Results (in units of $10^{-2}eV$ per electron) for eight trial wave functions are shown. The HF trial function has no Jastrow factor. The RPA1 trial function includes a Jastrow factor containing the homogeneous RPA u function from Eq. (5.2) but no χ. The RPA2 trial function uses the inhomogeneous RPA Jastrow factor derived in Section IV. For RPA1 and RPA2, the RPA cutoff k_c was $0.95a_0^{-1}$. The RPA3 trial function uses the inhomogeneous RPA Jastrow factor from Section IV, to which cusps have been added as explained in Section IV C. The RPA4 trial function uses the homogeneous RPA u function from Eq. (4.23) plus a χ function generated using Eq. (2.10). The Fourier cutoff k_n was $4.95a_0^{-1}$ in both cases. The EW trial function uses the Ewald-summed homogeneous u function from Eq. (5.3) and an analytic χ function calculated using Eq. (2.10). The VM1 trial function uses the same Ewald-summed homogeneous u function but a variance optimized χ. The VM2 trial function uses a variance optimized homogeneous u function and a variance optimized χ function.*

	HF	RPA1	RPA2	RPA3
E	-12.227(13)	-5.723(14)	-13.322(11)	-15.795(04)
σ	4.13	4.32	3.60	1.24
	RPA4	EW	VM1	VM2
E	-15.776(04)	-15.782(03)	-15.786(03)	-15.760(03)
σ	1.33	0.83	0.81	0.83